The 2025 World Congress on
Advances in Structural Engineering and Mechanics (ASEM25)
BEXCO, Busan, Korea, August 11-14, 2025

Consolidation Settlement Monitoring for Marine Reclamation Land of Incheon New Port using SBAS-InSAR Analysis

Jeongeun Kim[1)], *Inyoung Lee[2)], Lang Fu[3)], Sunil Cha[4)], Hyungjoon Seo[5)]

[1), 2), 4), 5)] *Department of Civil Engineering, Seoul National University of Science and Technology, Seoul 01811, Korea*
[3)] *Department of Civil and Environmental Engineering, University of Liverpool, UK L69 7ZX, UK*

[1)] *lkk109s@naver.com* [2)] *liy5984@naver.com* [3)] *L.Fu8@liverpool.ac.uk*
[4)] *tnsdlf37@gmail.com* [5)] *hjseo@seoultech.ac.kr* *(corresponding author)*

ABSTRACT

The reclamation site can experience ground settlement or instability because of construction and the surrounding environment during the reclamation period. Even after reclamation, continuous settlement occurs due to consolidation. The consolidation of the clay layer beneath the reclamation site can lead to long-term settlement over a wide area. However, existing technologies struggle to predict the timing and location of ground settlement, and in vast areas that are complexly subdivided, differing reclamation times pose significant challenges to assessing settlement comprehensively. In this study, the long-term settlement of the Incheon New Port reclamation area is monitored using Interferometric Synthetic Aperture Radar (InSAR) analysis. The reclamation site consists of various elements such as ground, structures, road pavement, and vegetation, which allows for the analysis of ground changes using Small Baseline Subset (SBAS) InSAR. Beneath the Incheon New Port, a clay layer extends over 20 meters, leading to predicted long-term consolidation settlement. This study analyzed a total of 88 datasets using Sentinel-1 at 12-day intervals from January 10, 2020, to December 31, 2022, using C-band. During the data analysis period, significant settlement was observed in the "New Port Hinterland," where reclamation was ongoing, with a maximum settlement of 243.3 mm confirmed through SBAS analysis. The Incheon New Port reclamation area was divided into 12 zones to assess the overall ground changes.

Keywords : ground settlement, consolidation, reclamation, SBAS-InSAR, Incheon New Port

---

[1), 2), 4)] Undergraduate Student
[3)] Ph.D Student
[5)] Associate Professor

1. INTRODUCTION

Consolidation-induced settlement of clay layers is a common phenomenon in coastal reclamation areas and alluvial plains (Xiaojie et al., 2019; Jiang et al., 2013). Unlike immediate settlement, consolidation settlement progresses over extended periods and can adversely impact surrounding buildings, roads, and underground infrastructure. As such, continuous monitoring is essential to ensure long-term structural stability (Nguyen et al., 2024; Qingwei et al., 2022).

In various countries, conventional geotechnical instrumentation has been widely employed to monitor consolidation settlement. For example, in Indonesia, settlement plates, inclinometers, and pore water pressure gauges were installed to monitor the settlement behavior of highways constructed on soft ground. The data were analyzed using Asaoka's method and Terzaghi’s one-dimensional consolidation theory (Undayani et al., 2023). Similarly, in Singapore, consolidation settlement in marine reclamation areas was monitored using a combination of field instruments, including piezometers, and analyzed through the Asaoka and hyperbolic methods. The degree of consolidation was primarily assessed based on pore water pressure trends (Arulrajah et al., 2007).

These traditional instrument-based methods are widely regarded for their high reliability, as they enable direct and quantitative measurement of settlement (Arulrajah et al., 2007). However, their major limitation lies in the point-based nature of data collection, which restricts the ability to capture the spatial variability of settlement over large areas (Jian et al., 2012). This issue becomes especially pronounced in large-scale reclamation projects, where ground deformation tends to be spatially heterogeneous. Even when multiple instruments are deployed, the spacing between them can limit representativeness and fail to detect local anomalies. For instance, in a reclamation project in Singapore, six settlement points within the same block exhibited final settlement differences of up to 82 cm, demonstrating significant spatial variation (Gong et al., 2021). Moreover, field-based monitoring systems require long-term maintenance, periodic calibration, and equipment replacement. Damage to sensors or disturbances during construction can result in data gaps and reduced reliability. These challenges highlight the need for a monitoring technique capable of covering large areas while maintaining high spatial and temporal resolution (Zhao et al., 2023). With advancements in satellite remote sensing, Interferometric Synthetic Aperture Radar (InSAR) techniques—particularly time-series methods such as SBAS-InSAR and PS-InSAR—have emerged as viable alternatives. These methods enable high-precision (millimeter-scale) monitoring of ground displacement across diverse environments, including urban areas, infrastructure sites, mines, slopes, and coastal wetlands (Li et al., 2024; Aswathi et al., 2022; Alonso et al., 2023). Since InSAR relies solely on satellite imagery, it facilitates non-contact, non-destructive, and wide-area monitoring without the logistical constraints of ground-based instrumentation (Xu et al., 2021).

In Iran’s Ardabil Plain, InSAR was used to monitor settlement induced by groundwater extraction and prolonged drought, revealing an average annual settlement rate of 45 mm and delineating spatial deformation patterns that would have been difficult to capture using field methods alone (Ghorbani et al., 2022). In South

Korea, similar applications have demonstrated the utility of InSAR in urban and port environments. In Incheon, InSAR successfully detected ground settlement around excavation sites, and in Busan Port, PS-InSAR was used to monitor settlement in reclaimed areas, effectively reducing survey costs while improving spatial resolution (Park et al., 2024; Ramirez et al., 2022). Among time-series InSAR methods, SBAS-InSAR is particularly effective for monitoring slow, progressive settlement in open areas, including reclaimed land and coastal clay layers, due to its ability to maintain stable interferometric signals even in vegetated regions (Guo et al., 2024). By selecting image pairs with short spatial and temporal baselines, SBAS-InSAR minimizes the effects of atmospheric artifacts and decorrelation noise (Xu et al., 2016). It processes multiple interferograms to generate reliable time-series data, making it highly suitable for detecting long-term consolidation-induced settlement.

In this study, the SBAS-InSAR technique was applied to the reclaimed land of Incheon New Port, South Korea, to detect and characterize surface settlement zones. The results were validated using borehole data and geotechnical investigations, enabling a comprehensive assessment of ground deformation across the study area. The findings demonstrate the capability of SBAS-InSAR to effectively monitor consolidation settlement in soft ground conditions, and its strong potential to serve as a foundational tool for future ground stability assessments and predictive settlement modeling in large-scale reclamation projects.

2. METHODOLGY

The SBAS-InSAR technique is a time-sequential InSAR technique based on a distributed target algorithm (Berardino et al., 2004). This method selects appropriate spatial baseline and temporal baseline thresholds to group the acquired SAR image sequences and form differential interferometric image pairs, and then selects coherent target points, removes atmospheric delays by spatial-temporal filtering, and obtains the deformation time series of the acquired surface by modelling and solving using a linear phase change model.

In the period T_0、T_1、$T_2 \ldots\ldots T_N$, N+1 images covering the same study area arranged according to the acquisition time sequence, according to the threshold requirement of the spatial-temporal baseline, all the images are freely combined to generate M differential interference pairs, and the relationship expression of the number of interference pairs M is as follows:

$$\frac{N+1}{2} \leqq M \leqq \frac{N(N+1)}{2} \tag{1}$$

Assuming that the two images imaged at the moments T_A and T_B, respectively, from the i^{th} interferometric pair ($T_A < T_B$), the interferometric phase difference of the coordinate point (x, y) under the radar coordinate system of this interferogram can be expressed as:

$$\delta\phi_i(x,y) = \phi_{T_A}(x,y) - \phi_{T_B}(x,y) \approx \delta\phi_{i(disp)} + \delta\phi_{i(topo)} + \delta\phi_{i(atmo)} + \delta\phi_{i(noi)} \tag{2}$$

where $\delta\phi_{i(disp)}$ is the deformation phase, $\delta\phi_{i(topo)}$ is the terrain phase, $\delta\phi_{i(atmo)}$ is the atmospheric phase and $\delta\phi_{i(noi)}$ is the noise phase. If only the deformation phase is retained for the time being, the equation can be simplified as follows:

$$\delta\phi_i(x,y) \approx \frac{4\pi}{\lambda}\left[d_{T_A}(x,y) - d_{T_B}(x,y)\right] \tag{3}$$

where λ is the radar microwave wavelength, $d_{T_A}(x,y)$ and $d_{T_B}(x,y)$ are the deformation of the coordinate (x,y) point at the T_A and T_B moments relative to the initial moment T_0. Assume that MI is the master image and SI is the slave image, and the corresponding M interference pairs are:

$$MI = [MI_1 MI_2 \dots MI_M] SI = [SI_1 SI_2 \dots SI_M] \tag{4}$$

the above equation satisfies $MI > SI$, where $\forall_i = 1,\dots,M$ Then for any interferogram, the following expression corresponds:

$$\delta\phi_i(x,y) = \phi\left(T_{MI_i}\right) - \phi\left(T_{SI_i}\right) \ i = 1,\dots,M \tag{5}$$

The above equation consists of a system of equations consisting of N unknowns M equations expressed in matrix form:

$$\delta\phi = A\phi \tag{6}$$

where, A is $M \times N$ matrix, for the small baseline set interior, when $M \geqq N$, the above equation can be solved by the least squares method; when $M < N$ between each subset, it will produce the rank loss equation, which needs to be solved by the singular value decomposition method to solve for the minimum paradigm to obtain the deformations.

The processing flow of SBAS-InSAR technology is shown in figure 1:

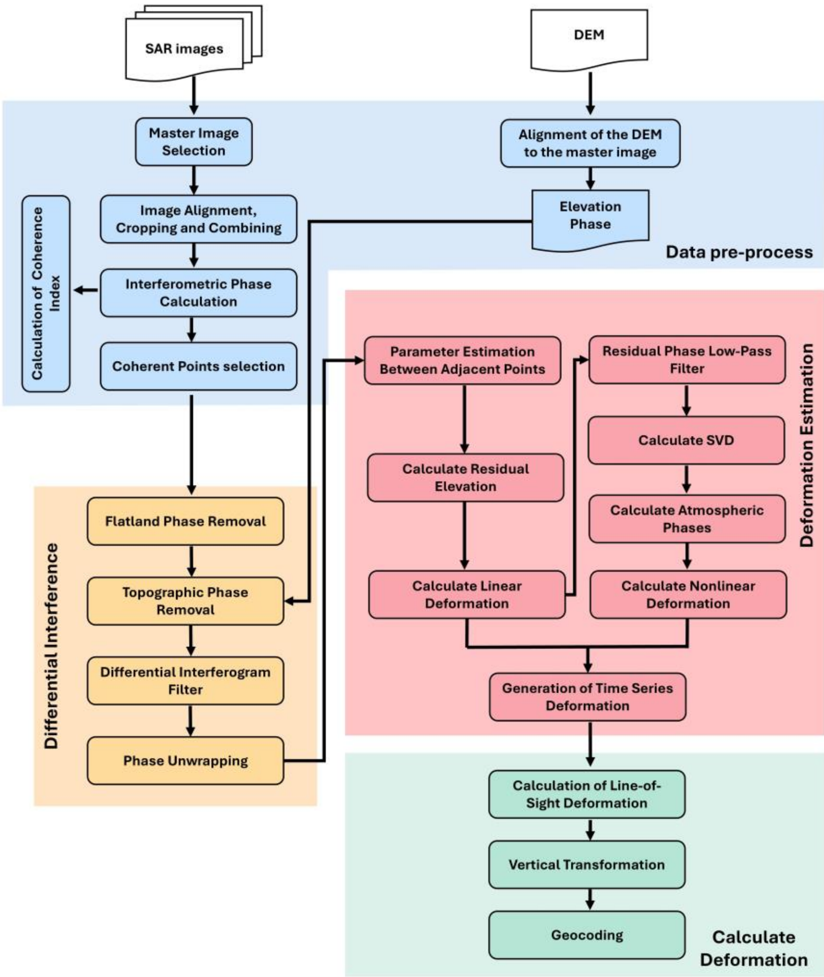

Figure 1. SBAS workflow

First, N+1 SAR images covering the study area are selected and combined into M interferometric pairs based on predefined spatial and temporal baseline threshold conditions. Using precise satellite orbital ephemeris data and an external digital elevation model (DEM), the flat-earth and topographic phase components are removed from each interferogram. Next, high-coherence targets are identified, and phase unwrapping and calibration are performed on the differential interferograms. Linear deformation and elevation error models are then established using these high-coherence targets. Finally, the deformation parameters are estimated using the least squares method and singular value decomposition (SVD). Nonlinear deformation and atmospheric phase components are separated, enabling the calculation of time-series ground deformation.

3. FIELD TEST

3.1 Introduction of site

This study aims to analyze time-series settlement in the reclaimed land of Incheon New Port, located in Incheon Metropolitan City, South Korea. The development of Incheon New Port was initiated to decentralize the operational load of

Incheon Port—the nation's second-largest trade port—and to accommodate large container vessels, thereby enhancing overall port capacity. The reclaimed area of Incheon New Port is subdivided into six primary sections: the LNG Receiving Terminal, Hinterland Complex Phases 1-1 and 1-2, and Container Terminal Phases 1-1, 1-2, and 1-3. As illustrated in Figure 2, several of these sections are further divided into zones based on reclamation periods. Specifically, the LNG Receiving Terminal and Hinterland Complex Phase 1-1 are each divided into three zones, while Container Terminal Phases 1-1 and 1-2 are each divided into two zones, resulting in a total of twelve zones across the study area. Reclamation activities began in 1993, starting with the LNG Receiving Terminal zone. As of 2025, reclamation is still ongoing, and portions of the site are being utilized as dredged soil disposal areas. The LNG Receiving Terminal includes liquefied natural gas (LNG) storage tanks and related infrastructure for the import and storage of LNG. The surrounding area also includes developed facilities such as parks, sports complexes, and golf courses. Zone 1 of Hinterland Complex Phase 1-1 houses a logistics complex, while the Container Terminal sections are equipped with berths and container yards for handling large vessels. In contrast, Zone 3 of Hinterland Complex Phase 1-1, all of Hinterland Complex Phase 1-2, and Container Terminal Phase 1-2 remain under active reclamation, indicating that both settlement behavior and land use vary across the different zones of Incheon New Port.

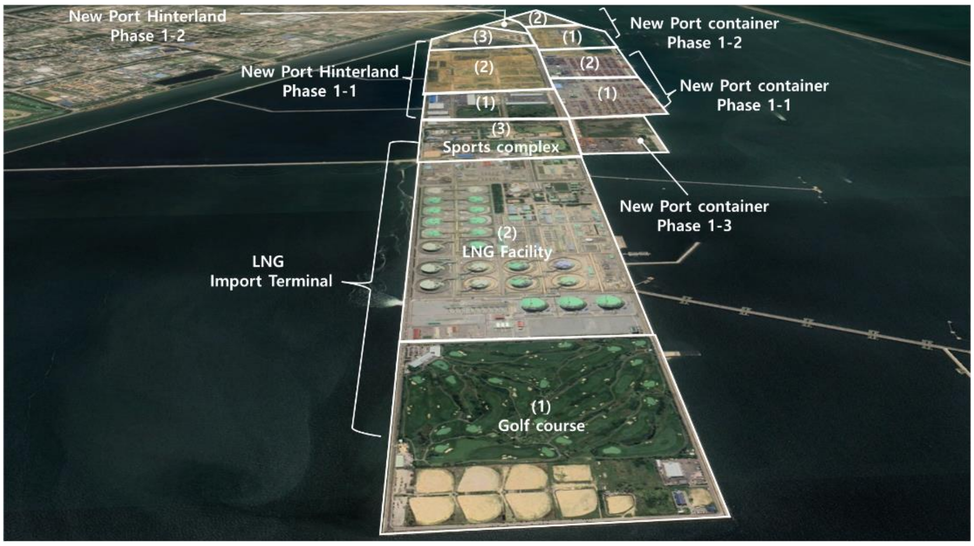

Figure 2. Master Plan of Incheon New Port

Table 1 summarizes the officially designated zones of Incheon New Port, their subdivision as used in this study, and the respective reclamation and construction periods. Zone 2 of the LNG Receiving Terminal was the first area within the Incheon New Port region to undergo reclamation, which commenced in 1993 and was completed in 1997. Following reclamation, LNG-related facilities were constructed within this zone. Using Zone 2 as a reference, adjacent Zone 3, located to the east, was reclaimed between 1996 and 2003 and has since been developed into a multi-purpose sports complex. To the west, Zone 1 began reclamation in 2001, which was completed in 2004, and a golf course was subsequently established in this area. In the hinterland area of Incheon New Port, Zone 1 of Phase 1-1 began reclamation in October 2017 and was completed by 2020. A logistics complex is currently under construction at this site. Zone 2 was used as a dredged soil disposal area starting in 2017, with reclamation completed in 2024. Zone 3 has served as a disposal site since 2021 and remains under active reclamation. Phase 1-2 of the hinterland has also been utilized as a disposal site since 2014, and reclamation activities are ongoing. Regarding the container terminal sections, Phase 1-3 began full-scale reclamation in 2021 following its initial use as a dredged soil disposal site starting in 2012. The final completion of reclamation in this area is scheduled for 2040. For the terminal-facing sections of Incheon New Port, Phase 1-1 commenced reclamation in 2009 and was completed in 2017. Afterward, terminal infrastructure was constructed, and the site became operational for large container vessels. To the east, Container Terminal Phase 1-2 has been used as a disposal site since 2014. Reclamation efforts accelerated in 2021 and remain in progress. During the reclamation process, rock materials were sourced from the Hyeongdo and Yangdo rock quarries near Incheon, selected for their availability, cost-effectiveness, and suitability for the construction schedule. The rock from Hyeongdo rock quarry had a specific gravity of over 2.58, water absorption less than 0.18%, and compressive strength ranging from 68.2 to 116.5 MPa. The rock from Yangdo rock quarry showed a specific gravity of over 2.62, water absorption less than 0.3%, and compressive strength ranging from 130.2 to 232 MPa. For sand materials, sand from Bukhansan Mountain was used during the reclamation. Laboratory tests confirmed the material met the quality standards for sand drains, with 2.19% passing the #200 sieve, D_{15} of 0.2 mm, D_{85} of 2.5 mm, and a permeability coefficient of 2.65×10^{-4} m/sec. For caisson sand filling and SCP foundation treatment, sand was obtained from a domestic supplier that had acquired the official permit for extraction of Bukhansan Mountain sand. In the dredged reclamation area, dredged fill material was used with the following properties: bulk unit weight of 18.9 kN/m², saturated unit weight of 18.9 kN/m², and cohesion of 9.8 kN/m².

Table 1. Zoning Information of Incheon New Port and Land Reclamation and Construction Information

Site	Position	Construction Time
Area1 (Point 1-5)	LNG Import Terminal (1) Golf Course	2001-2004
Area2 (Point 6-10)	LNG Import Terminal (2) LNG Facility	1993-1997
Area3 (Point 11-13)	LNG Import Terminal (3) Sports Complex	1996-2003
Area4 (Point 14-16)	New Port Hinterland phase 1-1 (1)	2017.10-2020.07
Area5 (Point 17-21)	New Port Hinterland phase 1-1 (2)	2021.08-2024.08 2017 : Dredged soil reclamtion
Area6 (Point 22-24)	New Port Hinterland phase 1-1 (3)	2024.11.27 (Conclusion of an Implementation Agreement) 2021 : Dredged soil reclamation
Area7 (Point 25)	New Port Hinterland phase 1-2	2024.11.27 (Conclusion of an Implementation Agreement) 2014 : Dredged soil reclamation
Area8 (Point 26-28)	New Port Hinterland phase 1-3	2021-2040 2012 : Dredged soil reclamation
Area9 (Point 29,30)	New port container phase 1-1 (1) Hanjin terminal	2009.04-2017
Area10 (Point 31,32)	New port container phase 1-1 (2) Sunkwang terminal	2009.04-2017
Area11 (Point 33,34)	New port container area phase 1-2 (1)	2021.08-2027. Second half of the year 2014 : Dredged soil reclamation
Area12 (Point 35)	New port container area phase 1-2 (2)	2015 : Dredged soil reclamation

Prior to the reclamation, a total of 65 boreholes were drilled across the site for geotechnical investigation, as illustrated in Figure 3a. Among these, 18 boreholes were drilled as part of a joint site investigation, while the remaining 47 were executed for foundation design purposes. The boreholes located within the study area include IF-1 through IF-5 and BN-1, 2, 3, 6, 7, 8, 9, and 39. According to Figure 3a, the section most relevant to the study area lies along the A–A' profile, where stratigraphic information from boreholes IF-1 and IF-2 is available. Figure 3b shows that weathered rock was encountered at a depth of 42.3 m in borehole IF-1, with a weathered soil layer distributed above it from 40.8 m to 42.3 m. The sandy soil layer spans depths of 20.1 m to 40.8 m, which is further subdivided into silty sand layers between 20.1–25.8 m and 33.3–37.8 m, and clean sand between 25.8–33.3 m and 37.8–40.8 m. Beneath the fill layer, a cohesive soil layer is present from 0.3 m to 20.1 m, consisting of silt from 0.3–3.5 m and silty clay from 3.5–20.1 m. In borehole IF-2, weathered rock was identified at 45.5 m. The sandy soil layer extends from 29.0 m to 45.5 m, comprising sand (29.0–33.5 m), silty sand (33.5–39.5 m), and sandy gravel (39.5–45.5 m). The cohesive soil layer beneath the fill extends from 1.5 m to 29.0 m, including silty clay (1.5–26.0 m) and silt (26.0–29.0 m). The thickness of the cohesive soil layer is approximately 19.8 m in IF-1 and 29.0 m in IF-2. Given this difference, the IF-2 location is expected to experience more significant and prolonged consolidation settlement than IF-1 due to the greater thickness of compressible cohesive materials. According to Table 2, the geotechnical properties of the natural ground are as follows: saturated unit weight of 18.1 kN/m³, void ratio of 1.01, specific gravity of 2.69, compression index of 0.36, and coefficient of consolidation of 3.97×10^{-3} cm²/sec.

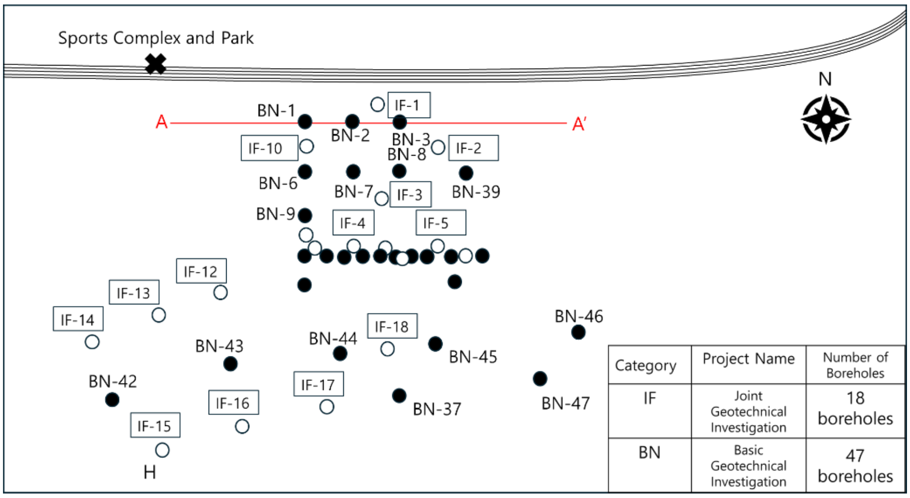

(a) Borehole Location Map of Incheon New Port

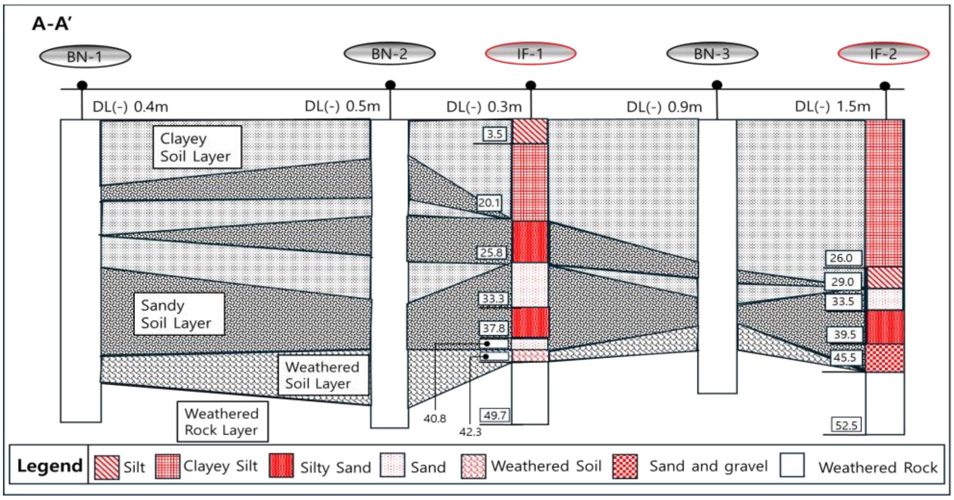

(b) Geological Cross-Section along Line A-A'

Figure 3. Results of Geotechnical Borehole Investigation at Incheon New Port

Table 2. Physical Properties of Native Soft Clayey Soil

Classification	Native Soft Clay
Water Content (w_n, %)	34.7
Specific Gravity (G_s)	2.69
Saturated Unit Weight (γ_{sat}, KN/m^3)	18.1
Initial Void Ratio (e_0)	1.01
Compression Index (c_c)	0.359
Strength Increase Rate (m)	0.20
Undrained Shear Strength (s_u, KN/m^2)	$3.59 \times z_m + 8.27$
Coefficient of Consolidation (c_v, cm^2/sec)	3.97×10^{-3}
Horizontal Consolidation Coefficient (c_h, cm^2/sec)	$2 \times c_v$
Overconsolidation Ratio (OCR)	Upper: 4.0, Lower: 1.8

In this study, the ongoing reclamation areas at Incheon New Port are being filled primarily with cohesive soils. Due to the high-water content of these materials compared to the original ground, they form extremely soft clayey ground, necessitating the implementation of ground improvement techniques designed for ultra-soft soils. As shown in Figure 4a, surface stabilization methods—such as the installation of wide horizontal drains and bottom mats—were applied to enhance ground stability and improve the drainage capacity of surface water in the early stages of reclamation. Following the placement of the bottom mat, a grid-type bamboo lattice was installed, which was subsequently overlaid with a sand mat to reinforce the upper ground surface. To facilitate the smooth dissipation of pore water generated during the consolidation process and to accelerate consolidation while lowering the groundwater table, horizontal drainage systems consisting of sand mats and bundled board drains were adopted. Additionally, as a countermeasure against excessive settlement, vertical drainage was implemented using prefabricated vertical drains (PVDs). As illustrated in Figure 4b, these plastic board drains were installed vertically into the soft ground to create effective drainage paths. This method was used in conjunction with lightweight reinforcement plates to enhance settlement adaptability and enable deep ground improvement, thereby promoting controlled consolidation settlement. To further reduce residual settlement, a preloading method was applied during the reclamation process. This involved vibration compaction as well as the use of surcharge blocks and gravel loads, as shown in Figure 4c. The surcharge embankment was constructed using dredged soil, which reduced the need for imported sand. However, since this dredged soil was sourced from marine excavation activities at Incheon New Port, its clay content renders it susceptible to long-term consolidation settlement. Despite the application of accelerated consolidation techniques (Figure 4) aimed at improving the soft ground and inducing rapid settlement in the hinterland reclamation areas, long-term settlement has continued to occur. Accordingly, the objective of this study is to evaluate the extent of consolidation-induced settlement in the reclaimed areas of Incheon New Port by applying the SBAS-InSAR technique.

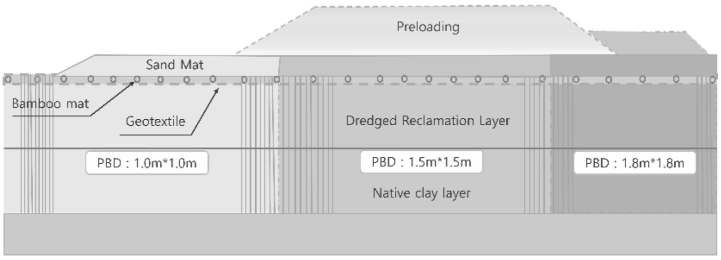

(a) Ground Improvement Methods

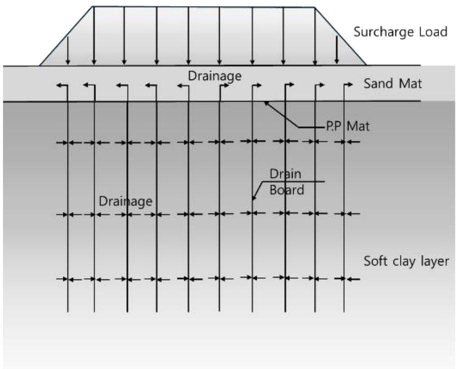

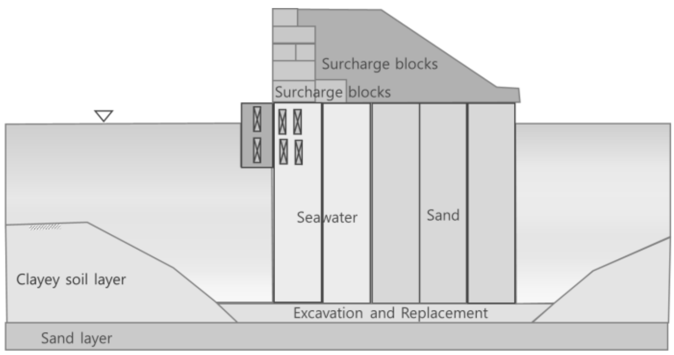

(b) PBD+Lightweight Reinforcement Plate (c) Conceptual Diagram of Preloading

Figure 4. Ground improvement techniques designed for ultra-soft soils

3.2 Data collection

In this study, the Incheon New Port area was subdivided into 12 distinct zones based on the reclamation timeline, as illustrated in Figure 5a. The study site was broadly categorized into two main sections: the northern section, encompassing the LNG Receiving Terminal and port hinterland, and the southern section, consisting primarily of quay facilities and terminal infrastructure. For the northern section, a 6,175.35-meter east–west transect was defined along the latitude 37°21′5.71″N, and approximately 25 monitoring points were established at intervals of 250–260 meters. In the southern section, which includes the terminal areas, 10 monitoring points were distributed along a 4,046-meter east–west transect centered on latitude 37°20′42.79″N. Considering both reclamation chronology and the spatial distribution of infrastructure, the site was divided into 12 zones. From west to east, Areas 1 through 7 constitute the northern section, while Areas 8 through 12 comprise the southern section. Figure 5b shows the monitoring points in the LNG import terminal area, spanning from Area 1 to

Area 3. Area 1 (Points 1–5) consists of vacant land and a golf course under the jurisdiction of the LNG Receiving Terminal. Area 2 (Points 6–10) contains LNG-related facilities such as storage tanks, factories, and a science museum. This area is the oldest reclaimed zone. Area 3 (Points 11–13) includes a multi-purpose sports complex affiliated with the LNG Terminal. Areas 4 to 7 correspond to the port hinterland, and the monitoring points can be identified in Figure 5c. Among these, Area 4 (Points 14–16) and Area 5 (Points 17–21) are developed zones. The remaining areas—Area 6 (Points 22–24) and Area 7 (Point 25)—are still undergoing reclamation. Figure 5d illustrates the distribution of monitoring points across Areas 8 through 12. In the southern section, area 8 (Points 26–28) is located on the western end of the quay. Area 9 (Points 29–30) includes the Hanjin Container Terminal. Area 10 (Points 31–32) comprises the Sun Kwang Terminal. Areas 11 and 12 are former dredged soil disposal sites, initiated in 2014 and 2015 respectively, with Area 11 corresponding to Points 33–34 and Area 12 to Point 35. To minimize the potential influence of ship traffic and docking activities typically concentrated near quay facilities, this study focused exclusively on the northern section (Areas 1–7) for settlement analysis. Particular emphasis was placed on Areas 4 through 7, where active reclamation and land development were ongoing during the monitoring periods.

(a) Zoning layout of Incheon New Port

(b) Point Locations from Area 1 to Area 3

(c) Point Locations from Area 4 to Area 7

(d) Point Locations from Area 8 to Area 12

Figure 5. Zoning layout of Incheon New Port and Designated Measurement Points

In this study, five satellite images from the years 2017, 2018, 2019, 2020, and 2023 were analyzed to assess the progress of land reclamation in Areas 4 through 7 and to track the overall development of the Incheon New Port. The temporal evolution of the reclamation process is visually represented in Figure 6. In the 2017 image (Figure 6a), Areas 1 through 3 had already undergone reclamation and development, with completed facilities such as the golf course and LNG Receiving Terminal clearly visible—consistent with the construction timelines presented in Table 1. At that time, Areas 4 and 5 were being utilized as dredged soil disposal sites, with partial land formation in progress. In the southern terminal area, Areas 8 and 9 were fully developed and operational, and container stacking activity was observed in Area 10. The 2018 image (Figure 6b) indicates continued reclamation activity in Areas 4 through 7, where the use of dredged material for land formation is evident. In the 2019 image (Figure 6c), the extent of reclaimed land in these zones had further expanded compared to 2018. By 2020 (Figure 6d), Area 4 was fully reclaimed, and significant reclamation progress was made in Area 5, although seawater remained in Area 6. In the most recent image from 2023 (Figure 6e), Areas 5 through 7 show near-complete reclamation, except for Area 6, where water remains. This is attributable to the designated development plan for Incheon New Port, which includes the creation of a lake in Area 6. Accordingly, complete land reclamation was intentionally excluded in that zone. Based on these observations, this study considers the reclamation of the northern section—particularly Areas 4 and 5—as effectively complete by 2020 (Figure 6d), and thus selected this year as the starting point for consolidation settlement analysis. Using the soil properties listed in Table 2 and applying Terzaghi's one-dimensional consolidation theory, the estimated settlement at borehole IF-1 was calculated to be 102.6 mm, with a corresponding final consolidation time of 7.83 years. In contrast, the estimated settlement at borehole IF-2 was 476.34 mm, with a final consolidation duration of 16.79 years. These results indicate that the magnitude of consolidation settlement at IF-2 is more than four times that at IF-1, while the settlement duration is more than twice as long. This disparity underscores the influence of clay layer thickness on both settlement magnitude and duration. Such spatial variability in subsurface stratigraphy introduces significant uncertainty in the behavior of reclaimed land, potentially resulting in long-term residual settlement. Therefore, to monitor and evaluate this long-term consolidation behavior, this study initiated satellite-based InSAR analysis beginning in 2020.

(a) 2017

(b) 2018

(c) 2019

(d) 2020

(e) 2023

Figure 6. Satellite images in New Port

3.3 SBAS processing

SAR data processing based on the SBAS (Small Baseline Subset) technique begins by constructing interferometric pairs from SAR images, which are then organized into a small baseline set. Interferometric connections are established based on constraints of a temporal baseline of 180 days and a spatial baseline of ±150 meters. As shown in the spatial-temporal baseline plot in Figure 7, all SAR images are effectively connected into valid pairs, with no isolated images or baselines exceeding the specified thresholds. Each line segment in the figure represents a master-slave image pair, indicating that an interferogram will be generated from that pair during the interferometric processing stage.

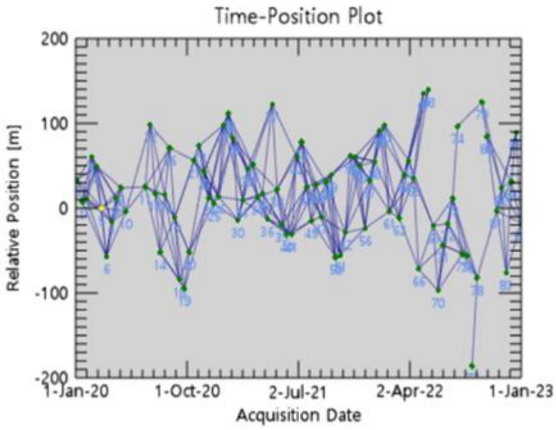

Figure 7. SBAS Time-Position Plot Graph

3.4 Annual interferogram

Figure 8 presents the SBAS-InSAR results in the form of interferograms, visualizing cumulative ground deformation relative to the initial observation date. Figure 8a displays the interferogram for the period from February 24, 2017, to December 31, 2022, based on 144 SAR images acquired over approximately six years. In the interferogram, red regions indicate ground uplift, while blue regions represent ground subsidence. The color scale denotes the annual average deformation rate, ranging from a maximum of +3.57 mm to a minimum of –7.95 mm. In Areas 1 through 4, including the LNG Receiving Terminal, uplift is observed—likely associated with structural loading and compaction due to construction. In contrast, Areas 5 and 6 remained under active reclamation, and due to persistent surface water coverage, interferogram formation was incomplete in many sections. Figure 8b illustrates the interferogram for the period from June 19, 2018, to December 31, 2022, derived from 120 images over five years. During this period, average deformation rates ranged from +7.86 mm to –14.46 mm. Similar to Figure 8a, SBAS analysis in Areas 5 and 6 was hindered by ongoing reclamation and residual water coverage. Nevertheless, substantial settlement signals were detected in the reclaimed zones, consistent with expected consolidation behavior. Figure 8c shows the interferogram generated using 100 images from June 14, 2019, to December 31, 2022. Compared to previous results, this interferogram covers a broader portion of Areas 4, 5, and 6, reflecting reclamation progress and reduced water presence. However, as also indicated in Figure 6c, unreclaimed sections remain, leading to incomplete interferogram coverage. During this period, ground deformation ranged from +13.87 mm to –30.01 mm, indicating an increase in settlement magnitude compared to earlier intervals. Figure 8d presents the interferogram for the period from January 4, 2020, to December 31, 2022, generated from 74 images. In Areas 1 through 3, where reclamation was completed earlier, deformation is minimal, reflecting stable ground conditions. In contrast, Areas 4 and beyond exhibit more intense deformation patterns. The widespread reduction of surface water in Areas 4 through 7 during this period allowed for near-complete interferogram coverage. Predominantly yellow hues indicate relatively stable ground, except in sections still undergoing settlement. The average deformation rate ranges from approximately +34 mm to –55 mm, representing the highest magnitude of ground movement observed across all time periods. This suggests that the most significant deformation occurred between 2020 and 2022. Given the availability of complete data and the pronounced settlement trends during this interval, the interferogram from 2020 to 2022 was selected for further analysis of ground deformation in the reclaimed zones of Incheon New Port.

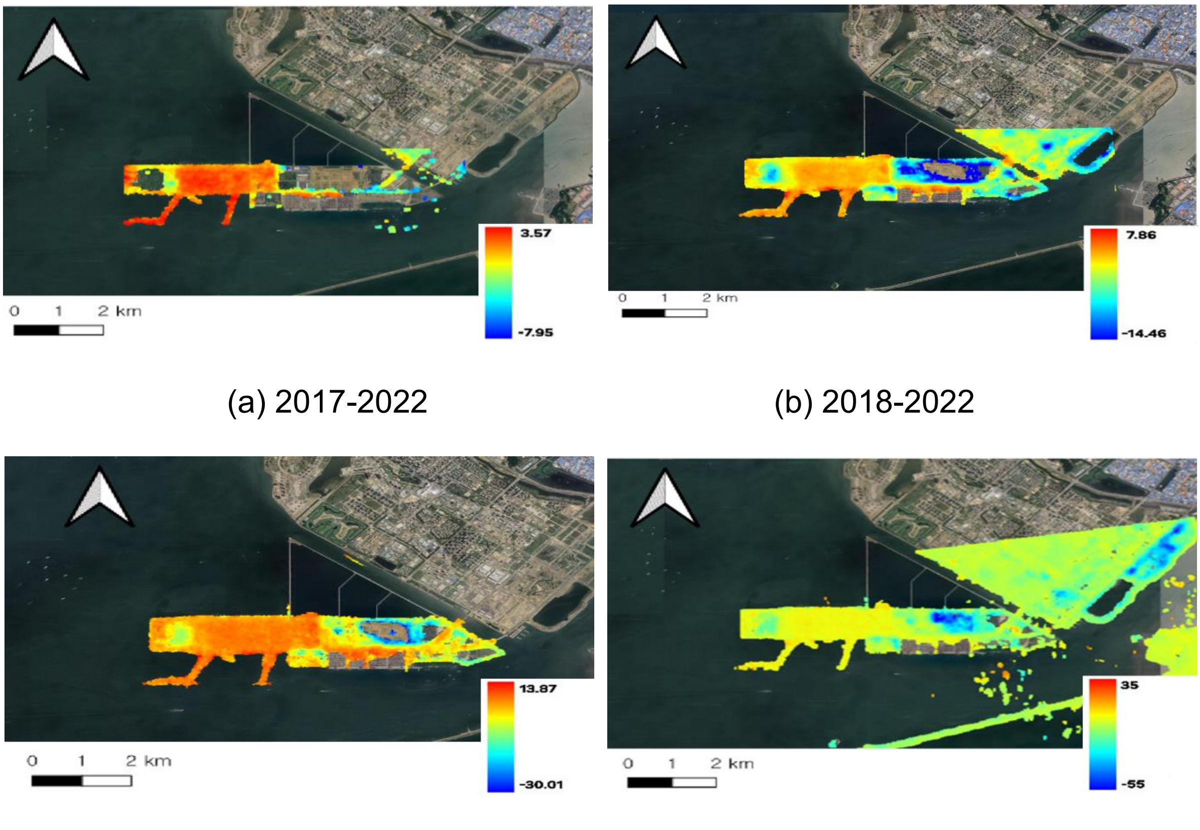

(a) 2017-2022 (b) 2018-2022

(c) 2019-2022 (d) 2020-2022

Figure 8. SBAS interferogram

3.5 Deformation rate graph

Figure 9 presents the time-series ground deformation results derived from SBAS-InSAR analysis at representative points located in Areas 1 through 7, as defined in Figure 5. Area 1 (Figure 9a) includes five monitoring points. The results exhibit a mixed pattern of both settlement and uplift. Over the three-year period (2020–2022), the maximum settlement was 49.0 mm, while the maximum uplift reached 21.5 mm. This irregular ground behavior may be attributed to the nature of the site, which includes a golf course and associated infrastructure. Areas 2 and 3 (Figure 9b) include eight monitoring points, all of which showed consistent uplift trends. The maximum uplift was 35.5 mm in Area 2 and 23.5 mm in Area 3. These areas contain LNG storage facilities and sports complexes, suggesting that minor ongoing construction activities may be contributing to gradual ground elevation. Area 4 (Figure 9c) includes three monitoring points, where ground settlement was generally observed. In particular, Point 15 showed a clear and continuous settlement trend, with a maximum cumulative deformation of 91.6 mm. This area, an undeveloped section of the port hinterland where vegetation is now present, completed its reclamation in 2020. Annual settlement at Point 15 was 67.1 mm in 2020, 15.0 mm in 2021, and transitioned to slight uplift of 3.8 mm/year in 2022—indicating that the most significant deformation occurred shortly after reclamation. Area 5 (Figure 9d) includes five points, all of which demonstrated consistent and substantial ground settlement. The maximum observed settlement was 243.3 mm. As shown in Figure 5c, Points 17, 18, and 19—located farther inland from the shoreline—exhibited the most severe deformation. Among them, Point 18 recorded the highest settlement: 136.8 mm in 2020, 54.2 mm in 2021, and 56.1 mm in 2022. This area has served as a dredged soil disposal site since 2017 and remains under reclamation until 2024, with no overlying infrastructure currently developed. Area 6 (Figure 9e) includes two analyzed points. Point 22 recorded a maximum settlement of 70.6 mm, while Point 24 exhibited 25.8 mm. The disparity is likely due to differences in ground composition—Point 24 lies on a roadway constructed in 1993, while Point 22 is situated within a recently reclaimed zone. SBAS-InSAR analysis was not feasible at Point 23 due to persistent water coverage and ongoing reclamation. Area 7 (Figure 9f) includes one point, which exhibited settlement behavior with a maximum deformation of 60.7 mm. The most substantial annual settlement occurred in 2020, reaching 38.0 mm/year. This point is also located within a dredged soil disposal site that has been active since 2014 and is still undergoing reclamation. In summary, the time-series analysis of Areas 1 through 7 demonstrates a general trend of settlement, with the most substantial deformation observed at Point 18 in Area 5. This point showed the highest cumulative settlement of 243.3 mm and the greatest annual settlement rate of 136.8 mm/year in 2020. These results indicate that Area 5 experienced the most significant ground deformation during the study period.

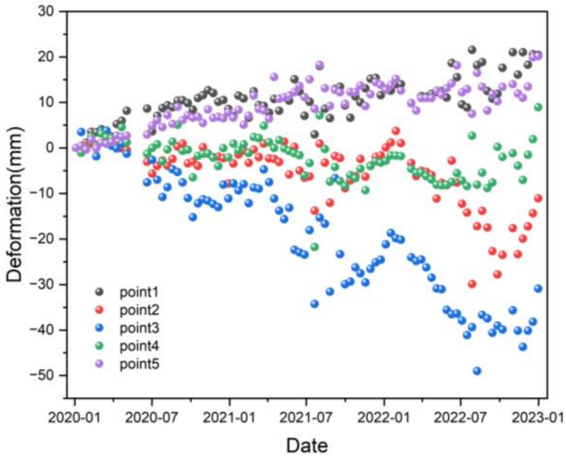

(a) Area 1

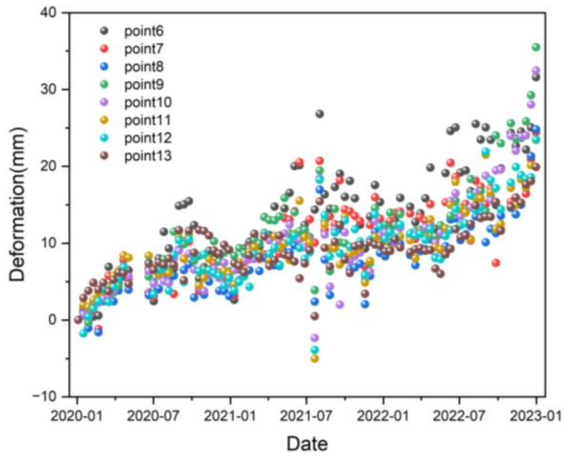

(b) Area 2&3

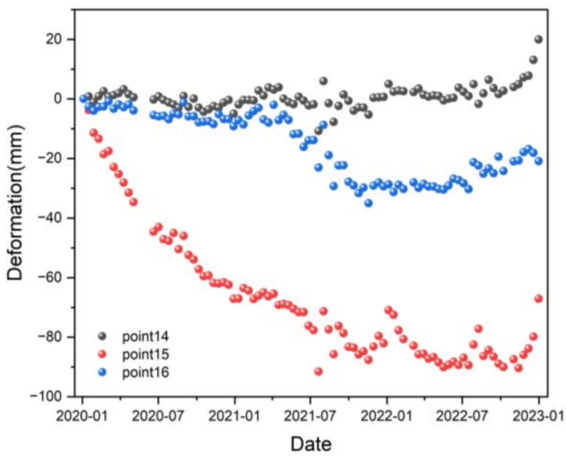

(c) Area 4

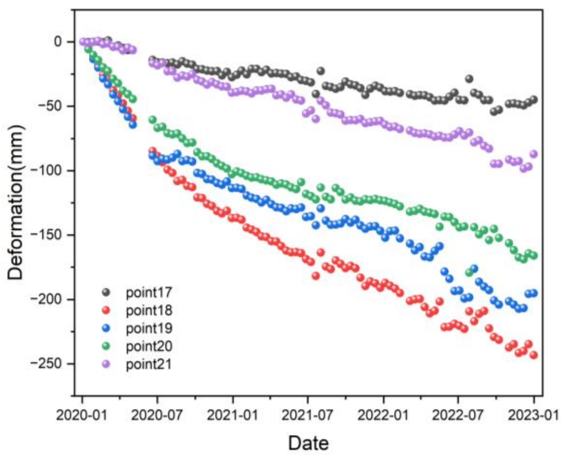

(d) Area 5

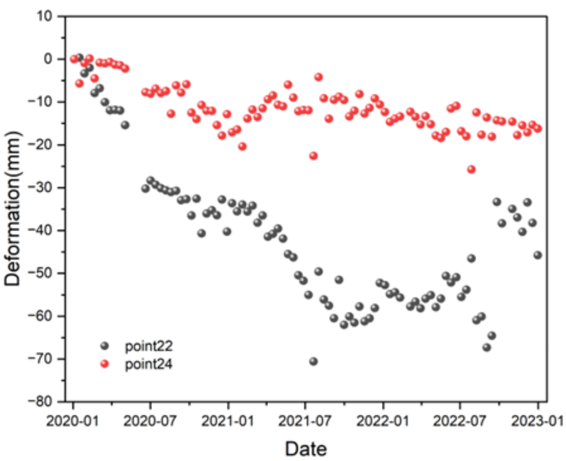

(e) Area 6

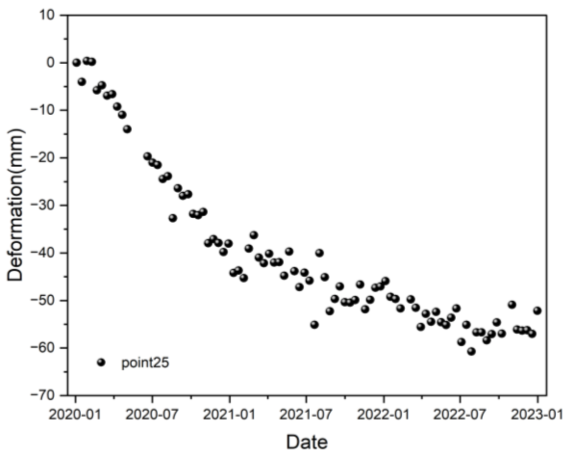

(f) Area 7

Figure 9. The Deformation-Time Graphs of new port in north.

Figure 10 presents the SBAS-InSAR time-series analysis results for representative monitoring points located in Areas 8 through 12, as defined in Figure 5d. Figure 10a shows the results for three points in Area 8, where a combination of ground settlement and uplift was observed. Over the three-year monitoring period (2020–2022), the maximum recorded settlement was 78.9 mm, while the maximum uplift reached 16.1 mm. Since Area 8 remains under active reclamation, the ground behavior varies by location, indicating non-uniform ground movement across the area. Figure 10b illustrates the time-series results for four points in Areas 9 and 10. These points showed a general trend of ground uplift. The maximum cumulative uplift in Area 9 was 33.6 mm, while Area 10 recorded a maximum of 31.2 mm. These areas include operational container terminals, and the observed uplift may be attributable to ongoing structural development, container stacking, and dynamic loading/unloading activities. Figure 10c presents the results for three points in Areas 11 and 12, all of which demonstrated settlement trends. The maximum settlement observed was 70.3 mm, with the most rapid change occurring in 2022, when the annual settlement rate reached 52.0 mm/year. According to Table 1, major reclamation activities in Area 11 began around August 2021, which accounts for the sharp increase in deformation during 2022. Area 11 is currently being developed for container storage, while Area 12, which has been used as a dredged soil disposal site since 2015, has no finalized development plan. As shown in Figure 6e, large portions of Area 12 remain submerged, and the presence of residual seawater affected the stability and continuity of the SBAS-InSAR signal, particularly for Point 35, resulting in inconsistencies in the time-series data. Among the southern waterfront zones (Areas 8 through 12), the greatest settlement was observed at a point 28 in Area 8, with a maximum cumulative deformation of 78.9 mm. Notably, most of the measurement points in these areas began to show a pronounced downward trend starting in 2022, indicating increased settlement during this period. Across all analyzed zones (Areas 1 through 12), the most substantial settlement occurred at Point 18 in Area 5, with a total deformation of 243.3 mm. This point also exhibited the highest annual settlement rate of 136.8 mm/year in 2020, confirming that the most significant ground deformation during the study period was concentrated in Area 5.

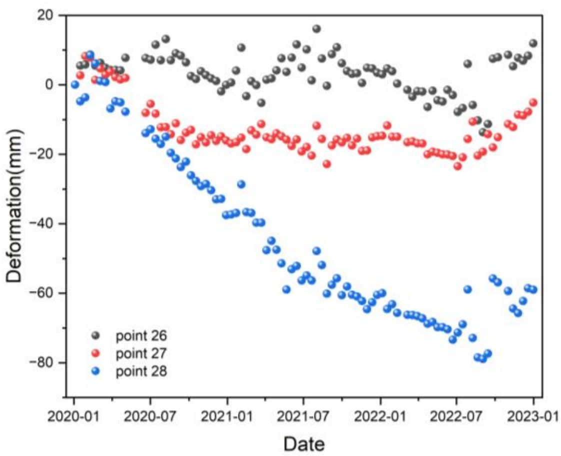

(a) Area 8

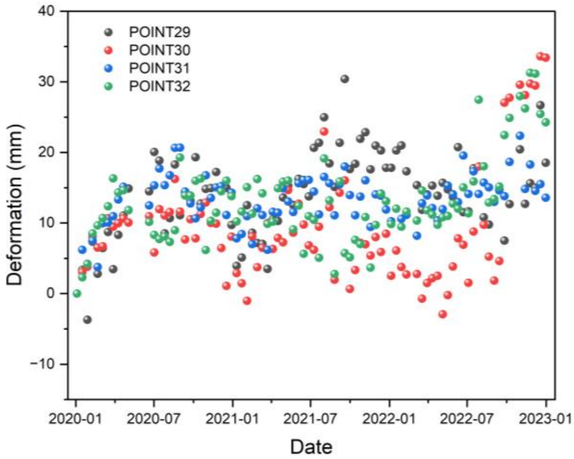

(b) Area 9&10

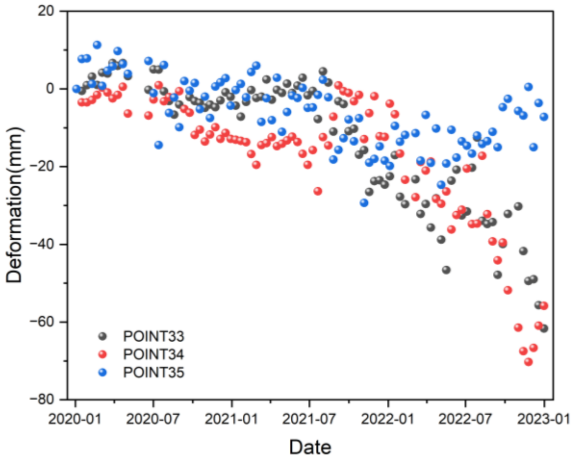

(c) Area 11&12

Figure 10. The Deformation-Time Graphs of new port in south.

4. DISCUSSION

Incheon New Port is a major hub for logistics and maritime transportation, where large-scale land reclamation has been ongoing since 1993. Due to the extended duration of development and the complex subdivision of the reclamation zones, accurately assessing ground stability across the entire port area poses considerable challenges. In particular, the presence of LNG storage tanks in the vicinity underscores the critical importance of ground stability, as any significant settlement could result in substantial economic and structural risks. Therefore, predictive and proactive management of ground deformation is essential.

To address the limitations of traditional assessment methods, this study applied the Small Baseline Subset Interferometric Synthetic Aperture Radar (SBAS-InSAR) technique to analyze consolidation-induced settlement in reclaimed zones of Incheon New Port.

The analysis results, as illustrated in Figures 9 and 10, indicate that the early-reclaimed areas showed a general trend of uplift between 2020 and 2022. This uplift is likely due to the gradual stabilization of the reclaimed ground over time, where internal structures that had previously undergone consolidation may have experienced rebound or heave as pore water pressures equilibrated and stresses were redistributed.

According to Table 2, the natural subsoil in the study area primarily consists of clay. To minimize the importation of sand, reclamation in these areas was largely performed using dredged soil for surcharge embankment. While various ground improvement techniques were applied, the presence of clay layers contributes to uncertainty in ground behavior and increases the likelihood of prolonged settlement.

The SBAS-InSAR analysis results highlight significant settlement trends in Areas 5, 6, 7, 11, and 12, as illustrated in Figures 9 and 10. According to the construction history outlined in Table 1, these zones were actively undergoing reclamation during the study period (2020–2022). Among them, Area 5 exhibited the greatest deformation, with a maximum cumulative settlement of 243.3 mm and a peak annual settlement rate of 136.8 mm/year in 2020. These values are consistent with site conditions; the observed settlement is most likely the result of consolidation within thick clay layers underlying the reclaimed fill.

Although this study successfully demonstrated the applicability of SBAS-InSAR for wide-area ground deformation monitoring at Incheon New Port, several limitations remain. Atmospheric disturbances, such as tropospheric delay, can introduce phase noise into the satellite data, leading to potential errors or data loss. Consequently, a more robust monitoring approach that reduces the influence of atmospheric artifacts is necessary to improve result reliability.

5. CONCLUSION

In this study, SBAS-InSAR was employed to analyze ground deformation at Incheon New Port over a three-year period from 2020 to 2022. At Incheon New Port, ground settlement was anticipated due to surcharge using dredged fill and the presence of cohesive clay layers in the natural subsoil. This is exemplified by borehole IF-2, which exhibited a total settlement of 476.34 mm with an estimated consolidation duration of 16.79 years.

For detailed analysis, Incheon New Port was divided into two principal sections—the northern port hinterland and the southern quay facilities—and further subdivided into 12 zones, encompassing a total of 35 measurement points.

Satellite images from the reclamation years of the port hinterland indicate that Areas 4 through 7 were actively undergoing reclamation, whereas Areas 1 through 3 had already been completed and developed with facilities such as a golf course and the LNG Receiving Terminal. In Area 10, container stacks were visible, reflecting ongoing terminal operations. These variations in land use and developmental stages contributed to the observed patterns of ground uplift and settlement in the interferogram analysis.

According to the SBAS interferogram analysis, the formation of interferograms was limited in areas with surface water. The 2020 to 2022 period exhibited the most pronounced ground deformation, and with substantial reclamation progress, the interferograms accurately represented the full spatial extent of Incheon New Port. During this interval, areas under reclamation experienced ground settlement, while other zones remained stable. The data from 2020 to 2022 were utilized for detailed, zone-by-zone settlement analysis in this study.

Based on the time-series analysis, the greatest settlement and highest annual settlement rate were observed at Point 18 in Area 5, with values of 243.3 mm and 136.8 mm/year, respectively, indicating that the most significant ground deformation occurred in 2020. The Deformation-Time Graphs showed that zones with completed construction exhibited upward trends, reflecting ground uplift, whereas areas undergoing active reclamation displayed pronounced settlement behavior.

This study demonstrates that SBAS-InSAR is an effective tool for monitoring long-term consolidation settlement in the reclaimed areas of Incheon New Port. Specifically, the time-series interferogram analysis from 2020 to 2022 enabled spatially comprehensive and quantitative assessment of ground deformation corresponding to various reclamation periods.

Acknowledgements
This work was supported by the National Research Foundation of Korea (NRF) grant funded by the Korea government (MSIT) (No. RS-2021-NR060085).

REFERENCE

Xiaojie Liu, Chaoying Zhao, Qin Zhang, Chengsheng Yang and Jing Zhang. (2019), "Characterizing and Monitoring Ground Settlement of Marine Reclamation Land of Xiamen New Airport, China with Sentinel-1 SAR Datasets", Remote Sensing, Vol. 11(5):585

Jiang, M.J., Zhang, N., Liu, J.D. (2013). "Compression Behaviors of Marine Clay for Coastal Reclamation in Dalian, China", (eds) New Frontiers in Engineering Geology and the Environment. Springer Geology. Springer, Berlin, Heidelberg.

Nguyen, N.T. (2024), "Long-Term Settlement Prediction for Over-Consolidated Soft Clay under Low Embankment", Engineering, Technology & Applied Science Research, Vol. 14(6), 18592–18599

Qingwei Chen, Zhen Yang, Binglei Xue, Zhipeng Wang, Dan Xie. (2022), "Monitoring and Prediction Analysis of Settlement for the Substation on Soft Clay Foundation", Intelligent Techniques for Structural Health Monitoring of Civil Engineering Structures, Vol. 2022(1).

Undayani Cita Sari, Sri Prabandiyani Retno Wardani, Agus Setyo Muntohar, Windu Partono and Kresno Wikan Sadono. (2023), "Consolidation settlement prediction and monitoring of toll road embankment at STA 23+650 Semarang–Demak Toll Road section", E3S Web of Conferences, Vol. 429(2023).

Arulrajah, A., Bo, M.W., Nikraz, H. and Balasubramaniam, A.S. (2007), "Geotechnical instrumentation monitoring of land reclamation projects on soft soil foundations", Common Ground, Vol. 2 :1–6.

Jian Chu, Indraratna, Shuwang Yan, Cholachat Rujikiatkamjorn. (2012), "Soft Soil Improvement Through Consolidation: An Overview", Proceedings of the International Conference on Ground Improvement & Ground Control, pp. 251–280.

Gong, W., Zou, H., Zhang, L., Cai, G., Liu, S. and Zhang, X. (2021), "Geostatistics-based spatial quality control of vacuum preloading in dredged materials", Proceedings of the 6th International Conference on Geotechnical and Geophysical Site Characterization (ISC'6), Budapest, Hungary (online), 26–29 September 2021.

Zhao J, Yang X, Zhang Z, Niu Y, Zhao Z. (2023), "Mine Subsidence Monitoring Integrating DS-InSAR with UAV Photogrammetry Products: Case Studies on Hebei and Inner Mongolia", Remote Sensing,Vol. 15(20):4998.

Li R, Gong X, Zhang G, Chen Z.(2024), "Wide-Area Subsidence Monitoring and Analysis Using Time-Series InSAR Technology: A Case Study of the Turpan Basin", Remote Sensing,Vol. 16(9):1611.

Aswathi, J., Binoj Kumar, R.B., Oommen, T., Bouali, E.H. and Sajinkumar, K.S. (2022), "InSAR as a tool for monitoring hydropower projects: A review", Energy Geoscience, Vol. 3(2),160–171.

Alonso-Díaz A, Casado-Rabasco J, Solla M, Lagüela S. (2023), "Using InSAR and GPR Techniques to Detect Subsidence: Application to the Coastal Area of "A Xunqueira" (NW Spain)", Remote Sensing, Vol. 15(15):3729

Xu, H., Chen, F. & Zhou, W. (2021), "A comparative case study of MTInSAR approaches for deformation monitoring of the cultural landscape of the Shanhaiguan section of the Great Wall", Heritage Science, 9, Article 71.

Ghorbani, Z., Khosravi, A., Maghsoudi, Y., Fazel Mojtahedi, F., Javadnia, E. and Nazari, A. (2022), "Use of InSAR data for measuring land subsidence induced by groundwater withdrawal and climate change in Ardabil Plain, Iran", Scientific Reports, Vol. 12(1): Article 13998.

Park, K., Kim, Y.J., Chen, J. & Nam, B.H. (2024), "InSAR-based investigation of ground subsidence due to excavation: a case study of Incheon City, South Korea", International Journal of Geo-Engineering,Vol. 15(1):article 26.

Ramirez, R.A. & Kwon, T.H. (2022), "Sentinel-1 Persistent Scatterer Interferometric Synthetic Aperture Radar (PS-InSAR) for Long-Term Remote Monitoring of Ground Subsidence: A Case Study of a Port in Busan, South Korea", KSCE Journal of Civil Engineering,Vol. 26(10), 4317–4329.

Guo J, Xi W, Yang Z, Huang G, Xiao B, Jin T, Hong W, Gui F, Ma Y (2024), "Study on Optimization Method for InSAR Baseline Considering Changes in Vegetation Coverage", Sensors, Vol. 24(15):4783.

Xu, Y., Zhu, W., Zhang, L. and Ding, X. (2016), "Coastal Subsidence Monitoring Associated with Land Reclamation Using the Point Target Based SBAS-InSAR Method: A Case Study of Shenzhen, China", Remote Sensing, Vol. 8(8) : 652.

Berardino, P., Casu, F., Fornaro, G., Lanari, R., Manunta, M., Manzo, M., Sansosti, E. (2004). "A quantitative analysis of the SBAS algorithm performance", IGARSS 2004. 2004 IEEE International Geoscience and Remote Sensing Symposium.